Optimization of random searches on regular lattices

M. C. Santos,[1] G. M. Viswanathan,[2] E. P. Raposo,[3] and M. G. E. da Luz[1,*]
[1]Departamento de Física, Universidade Federal do Paraná, 81531-990 Curitiba-PR, Brazil
[2]Departamento de Física, Universidade Federal de Alagoas, 57072-970 Maceió-AL, Brazil
[3]Laboratório de Física Teórica e Computacional, Departamento de Física, Universidade Federal de Pernambuco, 50670-901 Recife-PE, Brazil

(Received 22 June 2005; published 31 October 2005)

We investigate random searches on isotropic and topologically regular square and triangular lattices with periodic boundary conditions and study the efficiency of search strategies based on a power-law distribution $P(\ell)\sim\ell^{-\mu}$ of step lengths ℓ. We consider both destructive searches, in which a target can be visited only once, and nondestructive searches, when a target site is always available for future visits. We discuss (i) the dependence of the search efficiency on the choice of the lattice topology, (ii) the relevance of the periodic boundary conditions, (iii) the behavior of the optimal power-law exponent μ_{opt} as a function of target site density, (iv) the differences between destructive and nondestructive environments, and finally (v) how the results for the discrete searches differ from the continuous cases previously studied.

DOI: 10.1103/PhysRevE.72.046143 PACS number(s): 89.75.Fb, 05.50.+q, 05.40.−a, 89.75.Da

I. INTRODUCTION

The problem of finding randomly located target sites has applications in a large number of phenomena [1], such as biological searches for food or mates [2–10], which involves performing random walks in search spaces of dimension $d\leqslant 3$. Another potential area of application pertains to information theory [11] and regards the access to registers in high-performance databases. Furthermore, the problem of optimal well placement for oil recovery from older oil fields in geology can be approached in a similar manner [12].

Previous studies have focused on random searches in continuous Euclidean spaces [13–16]. However, in many potential technological applications, like in the Internet, discrete or digital rather than continuous search spaces may have greater relevance. For instance, this is the case for the question of memory search in neural networks [17]. Moreover, the exponentially increasing availability of information on integrated networked systems has rendered sequential searches over the entire information space covering all indexed devices impractical, if not impossible. Such difficulties have thus sparked interest in random search methods. Here, we turn our attention to random searches in lattice environments.

Experiments and numerical simulations [1,8–10,13,15,16] support the hypothesis that in the continuous case, processes defined by an asymptotic Lévy density distribution $P(\ell_j)\sim\ell_j^{-\mu}$, where P denotes the distribution of step lengths ℓ_j, lead to optimal random searches for particular values of $1<\mu<3$. The question is, then, how does the lattice topology affect the efficiency of an arbitrary (random or systematic) search? Consider the illustrative example of Internet search engines. The gathering of information typically is done by devices known as "crawlers." Recent results [18–21] suggest that the topological characteristics of a lattice affect the performance of the information search engines. In fact, a lot of effort has been put forward to determine which lattice structure would optimize the search, like in small-world dynamics [22] or in power-law network [21] contexts.

On the other hand, it is of practical relevance to understand what kind of random walks maximizes the search efficiency in a lattice of a given arbitrary topology. As a first step to tackle this general problem, we consider in this work regular lattices, more specifically square and triangular ones. By varying the value of the parameter μ of the asymptotic Lévy distribution, we study different types of search strategies on these lattice networks, comparing the results with the known optimal search strategies for continuous search spaces.

The paper is organized as follows. In Sec. II we define the problem and present the searching procedure. In Sec. III we report the numerical simulations. We discuss relevant aspects of the results in Sec. IV. Finally, in Sec. V we present our concluding remarks.

II. MODEL

We analyze the optimal strategies for a searcher that looks for randomly distributed target sites along regular, isotropic, and periodic square and triangular lattices, characterized by two quantities: the lattice parameter s (set equal to 1 in all the numerical simulations) and the coordination number k. The latter is the number of bonds leaving each node or, equivalently, the number of different directions that the search can follow from a given node. We have that $k=4$ (6) for the square (triangular) lattice.

We define a linear size $L=(\mathcal{N}-1)s$, with $\mathcal{N}$ denoting the number of nodes along the y direction. So the examples we discuss have a total area of $L\times L$ (square) and $\sqrt{3}L'/2\times L$ (triangular); see Fig. 1. Also, in the latter we distinguish two situations: the triangular ($L'=\mathcal{N}s$) and the nonergodic triangular (NE) ($L'=L$) lattices. Due to the relative number of nodes in the x and y directions, together with the periodic

*Electronic address: luz@fisica.ufpr.br

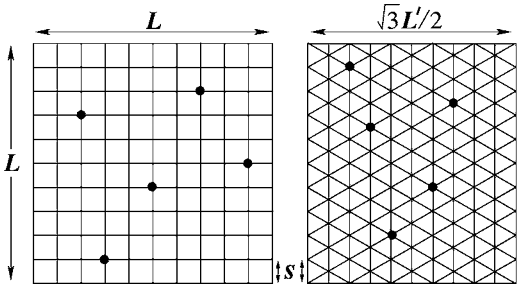

FIG. 1. Examples of the two types of lattices considered in this work. The dots at the nodes represent the randomly distributed target sites.

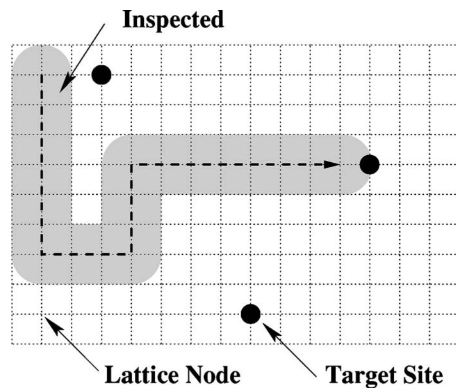

FIG. 2. Schematic representation of the searching dynamics. The gray regions indicate the area scanned by the forager during the flights. In this case $r_v = s$.

boundary conditions (BC's), for the first (second) case it is easy to show that if the forager leaves a given node along a certain direction not parallel to the x or y axis, always following straightforwarded towards it, then the forager will reach again this same node only after crossing all (at most two) lines of bonds parallel to the original direction.

Finally, we assume the targets are sparsely and homogeneously distributed along the nodes of the lattice. We consider two different types of search process: the destructive case, in which a previously visited target site becomes unavailable for subsequent visits, and the nondestructives case, when a visited site remains always available for future visits.

A. Lattice search dynamics

The ignorance about the exact locations of the target sites demands some type of probabilistic or statistical approach. On the other hand, the search process itself requires specific rules of locomotion, and hence an algorithmic dynamical procedure. Thus, at each step j of the search we consider the following rules:

(i) If there is a target site located within a "vision radius" distance r_v, reachable by moving along a straight line of bonds (i.e., no zigzag paths are allowed), then the forager detects it and moves to the site position.

(ii) If there are no target sites within a distance r_v, then the forager chooses one of the k possible directions at random and a distance ℓ_j (in units of s) from a probability distribution $P(\ell_j)$. It then incrementally moves to the new point, constantly looking for a target site within the distance r_v along its way (see Fig. 2). If it does detect a target site, it proceeds to the target site as in step (i). Otherwise, it stops after traversing the distance ℓ_j and chooses a new direction and a new distance ℓ_{j+1}.

(iii) In destructive searches a detected target site is immediately removed from simulation, becoming undetectable, and a new site is created at a random location [23]. In nondestructive searches a detected target site is immediately regenerated after the forager leaves its site.

The constraint against zigzags in rule (i) has no effect on the large-scale, only on the small-scale dynamics. Thus, we can impose such restriction and benefit from the reduction of the computational load. Also, notice that zigzags are forbidden within a single step ℓ_j. Variation of the parameter μ of the distribution $P(\ell_j)$ (see below) only has relevance if zigzags are absent within a flight. Nevertheless, this type of motion can arise via a probabilistic sequence of short flights (see Fig. 3).

Regular lattices have a metric which is similar to the continuous spaces: the farther a target site, the larger is the traveled distance to reach it. This is not true, for instance, for nonscaled small-world lattices, in which a single bond may connect two extremely distant nodes. Recent findings for continuous searches show in different situations [13–16] that random searches are more efficient if we assume power-law tails for the flight lengths (see Fig. 3)

$$P(\ell_j) \sim \ell_j^{-\mu}, \quad \ell_j > \ell_0, \tag{1}$$

leading to asymptotic Lévy walks, whose step lengths ℓ_j have no characteristic scale; i.e., the distribution has self-affine properties: $P(\lambda\ell) \sim \lambda^{-\mu} P(\ell)$, $1 < \mu \leqslant 3$. Gaussian (Brownian) behavior is a special case for $\mu > 3$. In the above expression, ℓ_0 is a typical lower cutoff distance, which in our case is set equal to r_v.

The reasons why such walks lead to the best efficiency are discussed in detail in Refs. [1,13,16]. Basically, they are related to the larger diffusion and smaller returning probability of Lévy processes, compared to the Brownian case. In spite of the fact that those conclusions are reached for Euclidean spaces in one, two, and three dimensions, we argue that the same reasoning can also be extended to regular lattices due to the already mentioned metric similarities. Thus, in our

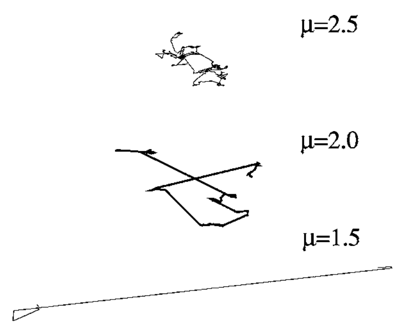

FIG. 3. Examples of Lévy flights on the two-dimensional plane for different values of μ.

analysis we assume Eq. (1) as our distribution $P(\ell_j)$ of step lengths, which are given by multiples of the net parameter s, such that $\ell_j = ns$, where n is a positive integer. Finally, it is worth mentioning that in the continuous case it has been shown [10] that some sort of zigzag behavior within a single Lévy flight does not alter the qualitative results from a pure Lévy walk. This is also true when short-range correlations are introduced [24].

B. Search efficiency

As discussed above, we have a family of distributions characterized by μ, corresponding to different search strategies. So a key point in the problem of random searches on regular lattices is to determine, for a given set of the system parameters, what is the optimal value for μ that maximizes the gain involved in finding search sites in the smaller total path (or time). To address this question we analyze the search efficiency $\eta(\mu)$, defined as the ratio of the number of visited target sites to the average total distance traversed [13] (average over M runs) or

$$\eta(\mu) = \frac{1}{M}\sum_{m=1}^{M} \frac{N_m}{L_m(\mu)}. \qquad (2)$$

Here, L_m is total distance traveled in the mth run to find N_m targets sites. In the simulations we take all the N_m to have the same fixed value N.

III. RESULTS

We discuss three types of lattices—square, triangular, and triangular-NE—and also two kinds of target sites—nondestructive and destructive. We also study how the efficiency varies with target site density. For the sake of comparison, in this section we use the same parameters values in all cases. We assume the lattice parameter $s=1$; the number of nodes, $\mathcal{N}=10^4$; the fixed number of target sites to be found per simulation, $N=500$; and a total of simulation runs for each lattice, $M=10^3$. We consider a number of target sites, N_t, of 10^3, 10^4, and 2×10^5 per lattice, corresponding to low, medium, and high densities, respectively. Also, we take $r_v=5$ for the low- and medium-target-density cases, but $r_v=50$ for the high-density case, to further enhance the probability of finding targets.

It is useful to define the quantity $\lambda = \mathcal{N}(\mathcal{N}+\chi)/(N_t 2 r_v/s)$, which roughly represents the mean distance (in units of s) between two target sites. Here, $\chi=0$ for square and triangular-NE lattices and $\chi=1$ for triangular lattices. The scaled efficiencies $\lambda\eta(\mu)$ as a function of μ are shown in Figs. 4–6. We should notice that, for the scaled efficiency, the high density can lead to lower values than those for the other two cases. This fact is just an artifact of this type of normalization. In Figs. 4 and 5 we have, respectively, the square and triangular lattices considering the different densities. The simulations for the triangular-NE lattices give essentially the same η as the triangular lattices for medium and high densities (so they are not displayed here). However, the results are different for low densities. In Fig. 6 we compare the efficiencies of our three type of lattices at this regime.

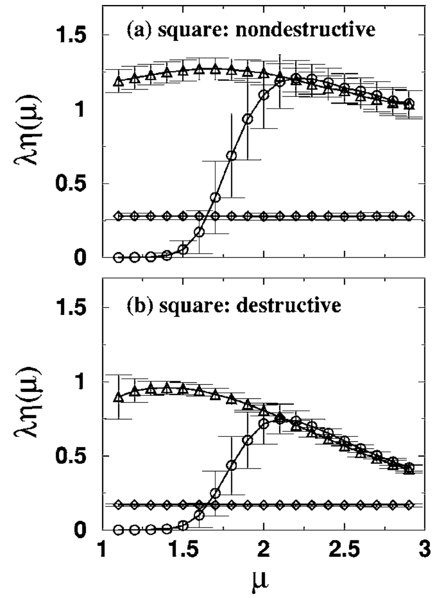

FIG. 4. The scaled efficiency $\lambda\eta(\mu)$ vs μ for square lattices. The circle, triangle, and diamond represent, respectively, low, intermediate, and high densities.

IV. DISCUSSION

In the remainder of this work we interpret the previous results and analyze the influence of the different features of our regular lattices to the search efficiency. We also discuss a number of issues, including the roles of target sites density, destructive and nondestructive targets, and lattice connectivity.

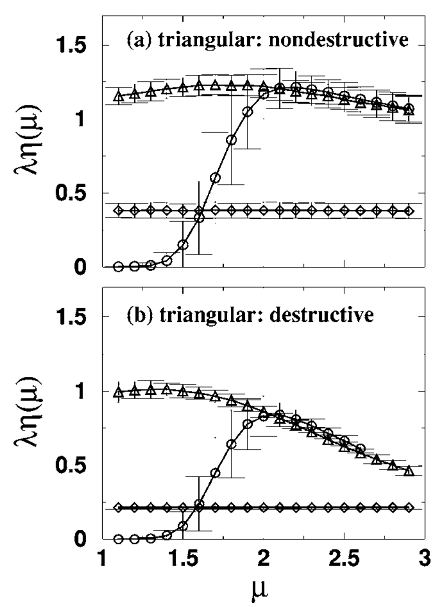

FIG. 5. The scaled efficiency $\lambda\eta(\mu)$ vs μ for triangular lattices. The circle, triangle, and diamond represent, respectively, low, intermediate, and high densities.

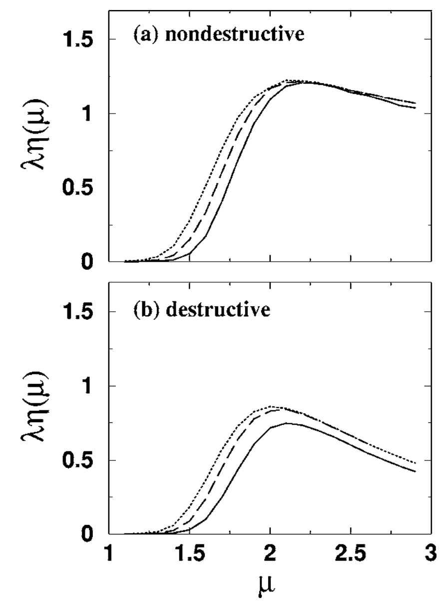

FIG. 6. The scaled efficiency $\lambda\eta(\mu)$ vs μ of the square (solid lines), triangular-NE (dashed lines), and triangular (dotted lines) lattices in the case of low density.

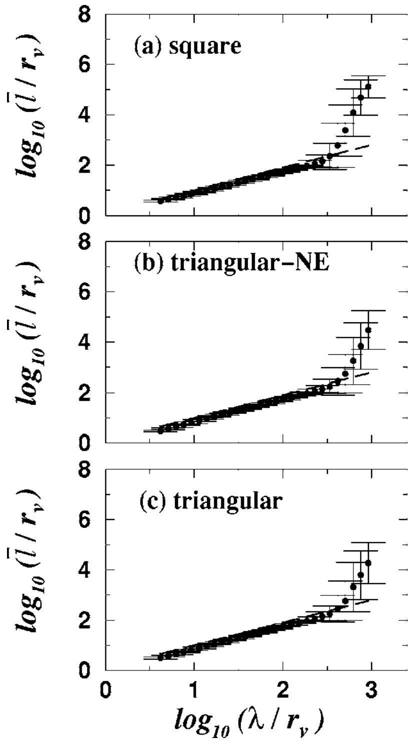

FIG. 7. The mean step $\bar{\ell}$ as function of λ/r_v in a log-log plot for the nondestructive case. For all the three lattices we take $\mu=1.1$, $r_v=5$, and $\mathcal{N}=10^4$ nodes in the y direction. The variation of λ is due to the variation of the number of target sites on the lattice. The dashed lines represent the analytical $\bar{\ell}(\lambda)$ expression discussed in the text.

A. Target site density

1. Low density

This situation is shown as circles in Figs. 4 and 5 and summarized in Fig. 6. We note that $\eta(\mu)\rightarrow 0$ when $\mu\rightarrow 1$. Furthermore, we find that $\mu_{\mathrm{opt}}\approx 2$ is the optimal exponent and η starts to diminish for larger values of μ. For low densities, we indeed expect the continuous limit and the relation between μ_{opt} and λ [13] to remain valid. To understand the global behavior we observe that the periodic BC's applied to regular lattices can generate in some cases a looplike trajectory for a single search step when the chosen ℓ_j is very large (recall that the flights larger than the system size are not truncated). If there are no target sites within r_v along the vicinity of such periodic orbit, then the searcher remains trapped in a loop until flight ℓ_j is fully traversed (for large densities the loops are unlikely to happen). This thereby reduces the search efficiency. One always can observe loops when the following three conditions are met: (i) low density of target sites, (ii) search strategy in long steps regime ($\mu<2$), and (iii) periodic BC's.

On the opposite limit of $\mu\geqslant 3$ (Brownian foraging), we have many small steps diffusing around the initial position. This phenomenon increases the total covered distance, therefore also diminishing efficiency. The maximum efficiency is a compromise between these two extremes, leading to $\mu_{\mathrm{opt}}\approx 2$, which is the same optimum value of the Euclidean continuous nondestructive search for low density [13,15].

2. Intermediate density

The numerical simulations for this case are represented by triangles in Figs. 4 and 5. Again we find that within the interval $1<\mu<3$ there is an optimum value for the exponent μ. This time, however, the values are always smaller than 2. The reason is that the intermediate densities of target sites are sufficiently large to truncate long steps $\ell_j\gg\lambda$, so distances greater than the characteristic lattices dimensions L are not traveled, suggesting that the searcher makes Lévy random walks truncated in λ. Since there is less need to return to previous sites, therefore lower values of μ get favored.

An important question which arises then is what is the critical value for λ—i.e., how small λ must be in order to truncate the search steps and so avoid looplike trajectories. We numerically investigate this point by fixing a small value for μ and then plotting on a log-log scale the average length for one step $\bar{\ell}$ divided by r_v as a function of λ/r_v. In such a graph we would expect a linear relation between these two quantities while truncation takes place. On the other hand, when truncation ceases, then $\bar{\ell}$ should present a rapid growth with respect to λ. Figure 7 corroborates these predictions, where we clearly identify the two regimes and the critical value for λ/r_v.

We obtain an analytical expression relating $\bar{\ell}$ and λ in the truncated regime from a very straightforward reasoning. For the linear part of the curves in Fig. 7, we can write

$$\bar{\ell}=A\left(\frac{\lambda}{r_v}\right)^B. \tag{3}$$

Now, we "borrow" a result valid for the Euclidean continuous case. There, the average length step in the truncated Lévy flights is given by [13,25]

$$\langle \ell \rangle \approx r_v \left(\frac{1}{2-\mu} \right) \left(\frac{\lambda}{r_v} \right)^{2-\mu} - r_v \left(\frac{\mu - 1}{2-\mu} \right). \quad (4)$$

For the situation we are discussing here, the first term on the right-hand side of the above equation is always dominant (supposing μ not too close to 2), so we can approximate $\langle \ell \rangle \approx r_v(2-\mu)^{-1}(\lambda/r_v)^{2-\mu}$. By directly comparing this last expression with Eq. (3), we find $A = r_v/B$ and $B = 2-\mu$. Using these parameters values, we reproduce the linear behavior in Fig. 7 quite well (dashed lines). So if the target density rises above a critical value, which for the examples shown in Fig. 7 is $\lambda/r_v \approx 300$, then the mean step can be approximated by the first moment of Lévy distribution truncated at λ.

3. High density

In the high-density limit, which basically corresponds to $\lambda \lesssim r_v$, a target site is quite often within the radius of vision. Hence, essentially all large steps are truncated and for each step one target site is almost always found irrespectively of lattice topology (triangular or square) and target properties (destructive or nondestructive). Therefore the efficiency has no dependence over μ, as seen from Figs. 4 and 5 (diamonds).

B. Destructive and nondestructive searches

Comparing the graphs shown in Figs. 4 and 5, we can see that the nondestructive are about 50% more efficient than the destructive searches. This difference arises because when the searcher leaves the nth found target site, but still remains near it, the searcher may probabilistically choose a possible step which will bring it back to such a site. In the destructive case, this will just increase the total distance traveled, without any gain in terms of number of found target sites.

This feature can be quantified by calculating the actual distance d_n traveled between the two successively found target sites $n-1$ and n, for $n=1,\ldots,N$. In Fig. 8 we show the distribution of such distances for $\mu=1.1$. We see that the distribution of d_n is concentrated around an average value, which is indeed larger for the destructive than for the nondestructive case. An interesting point to observe for the nondestructive case concerns the total number of sites that have a single compared to those that have multiple visitations at the optimal condition. The two values become approximately equal near μ_{opt}.

C. Lattice connectivity and boundary conditions

We first comment on our choice of BC's. We could have used not periodic but rather helical, absorbing, reflecting, etc., BC's. We avoided using absorbing BC's because they do not correspond to realistic random search phenomena. Reflecting BC's might find applications in the continuous case, but for networks and lattices periodic and helical BC's seem more plausible. Furthermore, reflecting BC's also have the drawback of taking the searcher back into recently visited sites. Thus, between helical and periodic BC's we have chosen the latter because they seem more representative for a general network system. Nevertheless, we have also run some simulations with helical BC's (not shown). Basically, they presented similar results, but we found that ultralong flights do not occur and so the optimal exponents values are closer to those of the continuous case (although not equal).

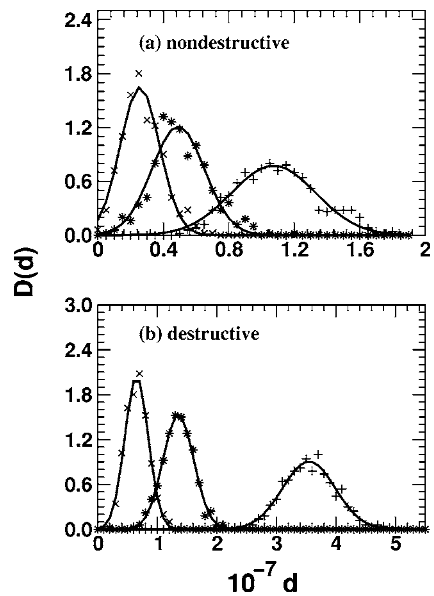

FIG. 8. Normalized distributions of the traveled distances between two successive found target for (+) square, (*) triangular-NE, and (×) triangular lattices. The parameters values are as in Fig. 6 for low density and $\mu=1.1$.

The only major differences between the triangular and square lattices are the coordination number k linking the sites and the effect of the periodic BC's. Regarding the BC's, as already pointed out, in the triangular case this type of periodicity does not give rise to loops; i.e., in a single very long step $\ell_j \gg L$ the searcher eventually could cover all the lattice nodes. On the other hand, for the triangular-NE and square cases, this is not possible. The lattice geometry is such that the searcher can be trapped in a loop during a single long step. Comparing results for triangular and square lattices, we find that in the former the distances covered between two successive sites are always smaller when the target sites are sparsely distributed—e.g., 4 times smaller for $\mu=1.1$ (see Fig. 8). So the triangular lattices lead to higher efficiencies than square ones for $\mu \to 1$. Notice that the triangular lattice has the highest efficiency. Similarly, we can expect that any BC's making the square lattice "more ergodic" (like the previous mentioned helical BC's) would increase its efficiency. Although intuitively one expects that a triangular lattice permits visitation of a greater number of target sites because of the larger number of connections, this feature is not relevant at a low-density regime. To exemplify this point, in Figs. 9(a) and 9(c) we show schematically a typical situation for triangular and square lattices at low density. Due to the small number of target sites, for $\ell_j = 5s$ and $r_v = 3s$ the extra possible directions of movement for the triangular lattice are not an advantage since only along a particular direction (represented by an arrow) will the searcher be able to scan the target. The other paths will not lead to such target site. In such a regime, however, the periodic BC's play a fundamental role. Note that low density requires small values for μ. It

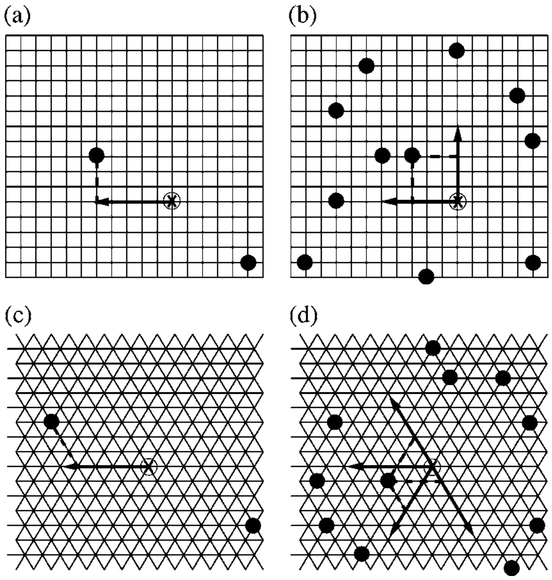

FIG. 9. Schematic representation of low- (a)–(c) and high- (b)–(d) density scenarios. For $\ell_j=5s$ and $r_v=3s$, the arrows represent the only steps which would lead to a target site.

represents ballistic behavior where loops occur frequently for squares and triangular-NE, hence diminishing their efficiency when compared to triangular lattices.

To test this hypothesis we consider a simulation of only one target site to be found N times by the searcher. We can then compute the return probability, which scales inversely to the distance ℓ_R covered before revisitation, so that we define $P=1/\ell_R$. To compare the performance in both types of lattices we numerically evaluate P_{tr}/P_{sq} in Fig. 10. We verify that the return probability is higher for triangular lattices. The loops for the square and triangular-NE lattices, especially for small values of μ, make the ℓ_R for such cases to become longer.

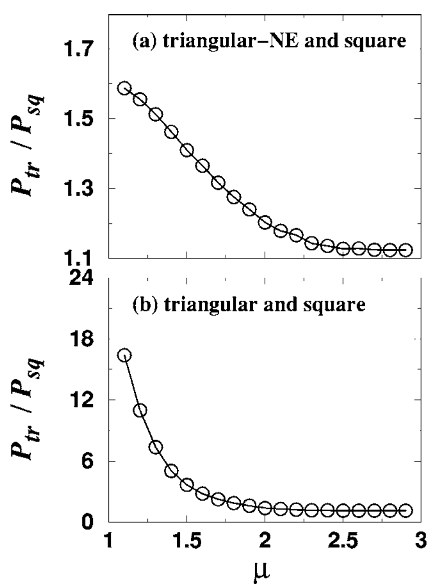

FIG. 10. The ratio between the returning probabilities for nondestructive triangular and square lattices as function of μ. Here we have $r_v=16$ and $\mathcal{N}=1000$.

In the opposite limit of high density, the triangular lattice has a little larger efficiency than that for the square one, a fact more pronounced in the nondestructive case (compare, for instance, Figs. 4 and 5). Observe that for high density loops practically do not occur. So it is the connectivity k which explains the larger mean and larger variance of the search efficiency for triangular lattices. Consider the schematic representation for such situation in Figs. 9(b) and 9(d). In the example, for the square lattice two out of four directions can lead to a given target, whereas for the triangular lattice four out of six directions can lead to a same target site. The higher variance arises due to the larger variation between the four path lengths, in comparison to the square lattice.

Finally, for intermediate densities we see from Figs. 4 and 5 that there are no important differences between the triangular and square lattices considering the whole range of μ. This can be understood by first observing that in this case the density is high enough to avoid loops. Indeed, for the parameters used we have $\lambda/r_v=200$, therefore below the critical value of 300 (see Fig. 7), above which loops start to take place. And second, the density is still low enough to prevent the effect of the connectivity to become relevant.

Last, we summarize the differences between continuous and lattice searches efficiencies. They are mainly due to the action of the periodic BC's. If we use truncated Lévy flights with a cutoff equal to the lattice size, then we expect behavior closer to the continuous case. Note that in continuous searches, looping is usually forbidden. So we have the following: (i) in lattices $\eta(\mu)\to 0$ when $\mu\to 1$ in sparsely distributed target sites, a consequence of the loops; (ii) triangular lattices appear less affected by BC's in this manner, yet the $\mu\to 1$ limit still leads to small efficiencies; (iii) no qualitative differences appear in the low-density regime between destructive and nondestructive searches in lattices, contrarily to what happens for searching in the continuous; and (iv) optimal strategies from the continuous space nondestructive case remain optimal also in lattice searches, even though for the destructive case a different optimal μ value arises.

D. Intermittent searches

Finally, we make a brief parallel between the present approach and the one recently proposed [26] to deal with hidden targets. It is a search strategy based on a "saltatory" (intermittent) behavior. The basic idea is that for difficult to find targets, the scanning mechanism should be a specialized process. So the random search would consist of two different procedures: a moving-only phase, when the searcher moves fast, changing from one location to another, and a second scanning only phase, during which the searcher explores its immediate vicinity, looking for the targets. Our model considers that during the moving process it is possible simultaneously to search for the target sites within a certain detection radius r_v. This is so in many concrete situations for the continuous case (see Refs. [1,2,13,14]) as well as for lattices when the targets are easy to identify—e.g., public websites on the Internet or register addresses in electronic databases. Of course, however, the method in Ref. [26] may be more appropriate in networks where the sites are somehow hidden. Thus, a future investigation along this line would be in order.

V. CONCLUSION

In summary, we have studied random searches on regular lattices and found that, as in continuous space searches, the optimal strategy depends on the target site density. For low density we have observed $\mu_{\rm opt} \approx 2$ as the optimal exponent. Increasing the density to intermediate values, we have found that μ going towards 1 becomes the more efficient strategy because long steps become truncated and the searcher effectively performs rectilinear ballistic motion between target sites. For high density all the strategies lead basically to the same result, so the exact value of μ no longer matters. We have also discussed the relevance of the coordination number k for the efficiency and its variance in the limit of high densities. We have revealed that periodic BC's lead to a number of interesting phenomena, such as higher than expected return probabilities in the triangular lattice, loops for low target density, etc. Those features lead to an unexpected similarity between the destructive and nondestructive efficiencies.

A natural continuation of this work should be the study of the effects of more general BC's—e.g., twisted node matches, as well as disordered lattices, e.g., due to broken links. Those are points which will be addressed in a future contribution.

ACKNOWLEDGMENTS

We thank CNPq, CNPq/Edital Universal, and FAPEAL for research grants and Professor Carlos Carvalho for technical computational support. M.G.E.d.L. also acknowledges grants from Finep/C T-Infra1 and CNPq/C T-Energ.

[1] G. M. Viswanathan, V. Afanasyev, S. V. Buldyrev, S. Havlin, M. G. E. da Luz, E. P. Raposo, and H. E. Stanley, Physica A **282**, 1 (2000).

[2] D. W. Stephens and J. R. Krebs, *Foraging Theory* (Princeton University Press, Princeton, 1987).

[3] A. C. Kamil, J. R. Drebs, and H. R. Pulliam, Eds., *Foraging Behavior* (Plenum Press, New York, 1987).

[4] M. Levandowsky, J. Klafter, and B. S. Whilte, Bull. Mar. Sci. **43**, 758 (1988).

[5] B. J. Cole, Anim. Behav. **50**, 1317 (1993).

[6] P. Nonacs and L. M. Lill, Oikos **67**, 371 (1993).

[7] F. L. Schuster and M. Levandowsky, J. Eukaryot Microbiol. **43**, 150 (1996).

[8] G. M. Viswanathan, V. Afanasyev, S. V. Buldyrev, E. J. Murphy, P. A. Prince, and H. E. Stanley, Nature (London) **381**, 413 (1996).

[9] F. Bartumeus, F. Peters, S. Pueyo, C. Marrasé, and J. Catalan, Proc. Natl. Acad. Sci. U.S.A. **100**, 12771 (2003).

[10] F. Bartumeus, M. G. E. da Luz, G. M. Viswanathan, and J. Catalan, Ecology **86**, 3078 (2005).

[11] P. Pirolli and S. Card, in *Proceedings of the 1995 Conference on Human Factors in Computing Systems*, edited by Gerrit C. van der Veer and Carolyn Gale (ACM Press, New York, 1995), pp. 51–58.

[12] F. A. L. Dullien, *Porous Media—Fluid Transport and Pore Structure* (Academic Press, New York, 1979); M. Sahimi, *Flow and Transport in Porous Media and Fractured Rock* (VCH, Boston, 1995).

[13] G. M. Viswanathan, S. V. Buldyrev, S. Havlin, M. G. E. da Luz, E. P. Raposo, and H. E. Stanley, Nature (London) **401**, 911 (1999).

[14] F. Bartumeus, J. Catalan, U. L. Fulco, M. L. Lyra, and G. M. Viswanathan, Phys. Rev. Lett. **88**, 097901 (2002).

[15] E. P. Raposo, S. V. Buldyrev, M. G. E. da Luz, M. C. Santos, H. E. Stanley, and G. M. Viswanathan, Phys. Rev. Lett. **91**, 240601 (2003).

[16] M. C. Santos, E. P. Raposo, G. M. Viswanathan, and M. G. E. da Luz, Europhys. Lett. **67**, 734 (2004).

[17] S. Nara, P. Davis, and H. Totsuji, Neural Networks **6**, 963 (1993).

[18] L. A. Adamic, R. M. Lukose, A. R. Puniyani, and B. A. Huberman, Phys. Rev. E **64**, 046135 (2001).

[19] R. Pastor-Satorras, A. Vazquez, and A. Vespignani, Phys. Rev. Lett. **87**, 258701 (2001).

[20] R. Guimera, A. Diaz-Guilera, F. Vega-Redondo, A. Cabrales, and A. Arenas, Phys. Rev. Lett. **89**, 248701 (2002).

[21] A. Vazquez, R. Pastor-Satorras, and A. Vespignani, e-print cond-mat/0206084.

[22] D. J. Watts and S. H. Strogatz, Nature (London) **393**, 440 (1998).

[23] Such a technical procedure of creating a site at random in the destructive case is used just to make the averages always with the same target density.

[24] M. G. E. da Luz, S. V. Buldyrev, S. Havlin, E. P. Raposo, and G. M. Viswanathan, Physica A **295**, 89 (2001).

[25] S. V. Buldyrev, S. Havlin, A. Ya. Kazakov, M. G. E. da Luz, E. P. Raposo, H. E. Stanley, and G. M. Viswanathan, Phys. Rev. E **64**, 041108 (2001).

[26] O. Bénichou, M. Coppey, M. Moreau, P.-H. Suet, and R. Voituriez, Phys. Rev. Lett. **94**, 198101 (2005).